Abrasion regimes in fluvial bedrock incision

Alexander R. Beer[1,2]* and Michael P. Lamb[1]
[1]Division of Geological and Planetary Sciences, California Institute of Technology, Pasadena, California 91125, USA
[2]Department of Geosciences, University of Tübingen, D-72076 Tübingen, Germany

ABSTRACT

River incision into bedrock drives landscape evolution and couples surface changes to climate and tectonics in uplands. Mechanistic bedrock erosion modeling has focused on plucking—the hydraulic removal of large loosened rock fragments—and on abrasion—the slower fracturing-driven removal of rock due to impacts of transported sediment—which produces sand- or silt-sized fragments at the mineral grain scale (i.e., wear). An abrasion subregime (macro-abrasion) has been hypothesized to exist under high impact energies typical of cobble or boulder transport in mountain rivers, in which larger bedrock fragments can be generated. We conducted dry impact abrasion experiments across a wide range of impact energies and found that gravel-sized fragments were generated when the impact energy divided by squared impactor diameter exceeded 1 kJ/m². However, the total abraded volume followed the same kinetic-energy scaling regardless of fragment size, holding over 13 orders of magnitude in impact energy and supporting general abrasion law. Application to natural bedrock rivers shows that many of them likely can generate large fragments, especially in steep mountain streams and during large floods, transporting boulders in excess of 0.6 m diameter. In this regime, even single impacts can cause changes in riverbed topography that may drive morphodynamic feedbacks.

INTRODUCTION

Bedrock river evolution shapes mountain regions and propagates changes in tectonics and climate throughout the landscape. Bedrock incision is most often modeled using the stream-power model (Whipple, 2004); however, this model does not explicitly represent rock erosion processes (Lague, 2010). Field observations and laboratory experiments indicate two main river erosion processes, plucking and abrasion (Wende, 1999; Whipple et al., 2000; Chatanantavet and Parker, 2009; Lamb et al., 2015). Plucking, the hydraulic removal of large, fractured rock pieces, is a highly efficient mechanism where shear stresses exceed a block entrainment threshold (Miller, 1991; Whipple et al., 2000; Lamb et al., 2015). In contrast, abrasion is the slower mass removal from massive rock through the creation and coalescence of fractures from impacting sediment that eventually liberate fragments (Sklar and Dietrich, 2004; Chatanantavet and Parker, 2009; Beer et al., 2017).

Abrasion has been proposed to be further divided into wear (incremental, grain-by-grain abrasion) and macro-abrasion (block fracture and chipping; Whipple, 2004). However, it remains unclear whether two distinct abrasion regimes exist, and if so, whether erosion rate laws differ for these regimes. For instance, Chatanantavet and Parker (2009) envisioned macro-abrasion as a process whereby particle impacts generate large rock fragments that can be removed via plucking, leading to an erosion rate formulation distinct from wear. Sklar and Dietrich (2004), in contrast, did not distinguish between wear and macro-abrasion and argued their abrasion relation should hold across a wide range of impact energies. Even if a universal abrasion law exists, distinguishing between wear and macro-abrasion regimes may be useful, because fragment size can influence sediment supply and morphodynamic feedbacks in channel evolution (Fig. 1A).

Significant insight into river abrasion has come from controlled experiments (Sklar and Dietrich, 2001; Scheingross et al., 2014; Small et al., 2015), but typically under relatively low impact energies, and fragment sizes were not reported in those studies. There are standardized geotechnical studies on fracturing and crack growth in brittle industrial materials (Atkinson, 1987; Hutchings and Shipway, 2017), but it is unclear whether these can inform fragment sizes generated in riverbeds. Despite the lack of macro-abrasion experiments, there are ample field observations of chipping at edges and fragment removal from massive rock (pieces exceeding 0.1 m), especially in rivers transporting cobbles and boulders that impact with significant force (Tinkler, 1993; Wende, 1999; Whipple et al., 2000; Hartshorn et al., 2002; Lamb and Fonstad, 2010; Beer et al., 2017). Because large grain impacts cause the greatest energy transfer to the bed (Turowski et al., 2015), macro-abrasion may be a major driver of bedrock river evolution.

We used laboratory experiments to explore erosion and fragmentation in massive rock over a wide range of impact energies to test for the onset of macro-abrasion and to evaluate the erosion rate law in the macro-abrasion regime. We hypothesized that previous experiments did not report fragments because of small impact energies that limited their sizes ($<10^{-5}$ J; Head and Harr, 1970; Engel, 1978; Sklar and Dietrich, 2001; Scheingross et al., 2014), as compared to boulder impacts in mountain rivers measured at 10^2 J (Turowski et al., 2013).

METHODS

Our experiments produced large impact energies by dropping gravel and cobbles onto concrete rock slabs through air, which has less drag than water (Fig. 1B). Although water-transported grains have ballistic trajectories due to saltation (Sklar and Dietrich, 2004), abrasion rates are modeled using the vertical component of their impact velocity (Bitter, 1963; Engel, 1978; Lamb et al., 2008). Thus, our experiments provide a direct comparison to abrasion theory. Moreover, viscous damping of impacts by water is negligible for gravel (Lamb et al., 2008; Scheingross et al., 2014), so drops through air should not have affected the results.

We conducted seven experimental sets varying rock strength, impactor size, and drop height to achieve a range of impact energies, while

---

*E-mail: alexander.beer@uni-tuebingen.de

[1]Supplemental Material. Additional details on the experimental methods, experimental data, Figs S1–S3, and Tables S1–S3. Please visit https://doi.org/10.1130/GEOL.S.13708303 to access the supplemental material, and contact editing@geosociety.org with any questions.
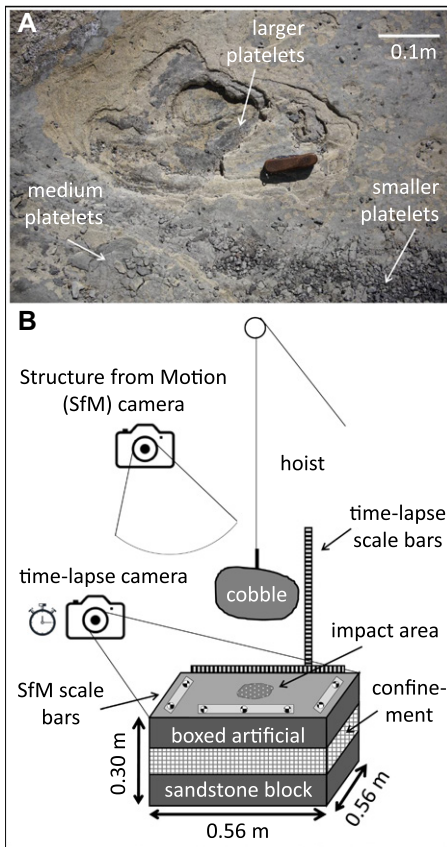
Figure 1. (A) Field example of macro-abrasion with different sizes of platelet-shaped sandstone fragments (Matalija Creek, California, USA). 9-cm-long folded knife for scale. (B) Sketch of macro-abrasion drop experiment setup, showing hoisted cobble that will impact an artificial sandstone block; schematic not to scale. Measured variables are defined in Figure S1A (see footnote 1), and sets of drop experiments are summarized in Table S1.

holding other variables equal (Table S1 in the Supplemental Material[1]). The impactors were semirounded, granitic river gravels (impactor diameter, D_i, = 46–170 mm). Some experiments used repetitive impacts from the same impactor; others used a mixture of up to 21 impactors of similar size. Targets were four homogeneous concrete blocks of two different tensile strengths (σ_t = 1.32 and 2.34 MPa; composed of 0.2 mm sand and cement), laterally confined to resemble infinite massive bedrock (see the Supplemental Material; Fig. 1B). Although fracturing in natural bedrock also depends on preexisting heterogeneities and weathering (Hancock et al., 1998; Scott and Wohl, 2019), our experiments focused on fracturing from impacts.

We used a high-speed camera to measure the kinetic energy of the impactor, ε_{imp}, and its rebounding energy, ε_{reb}, and differenced these to find the effective impact energy, $\varepsilon_{kin} = \varepsilon_{imp} - \varepsilon_{reb}$ (i.e., the energy lost during a collision due to abrasive work; see the Supplemental Material and Fig. S1). We measured total abraded bedrock volumes, V_a, by vertically differencing re-

peated millimeter-accurate topographic surveys of the blocks (see the Supplemental Material). We collected abraded gravel-sized fragments exceeding 2 mm in their largest axis, calculated the mean fragment volume per experiment, $V_{frag.mean}$, as the total volume of such fragments liberated, V_{frag}, divided by their number, n_{frag}, and calculated a representative average fragment diameter as $D_{frag.mean} = 2(3/4\ V_{frag.mean}/\pi)^{1/3}$.

We further compiled data from previous abrasion experiments, which spanned erosion by bed load and suspended load of natural rock, concrete, and foam (Head and Harr, 1970; Liu, 1981; Sklar and Dietrich, 2001, 2004; Scheingross et al., 2014), and calculated mean effective single-grain impact energies, ε_{kin}, and mean abraded volumes, V_a (see the Supplemental Material and Table S2). These studies did not report fragment sizes, but their descriptions are generally consistent with wear, e.g., sand grains liberated through fracturing of matrix cement. To investigate the potential of macro-abrasion
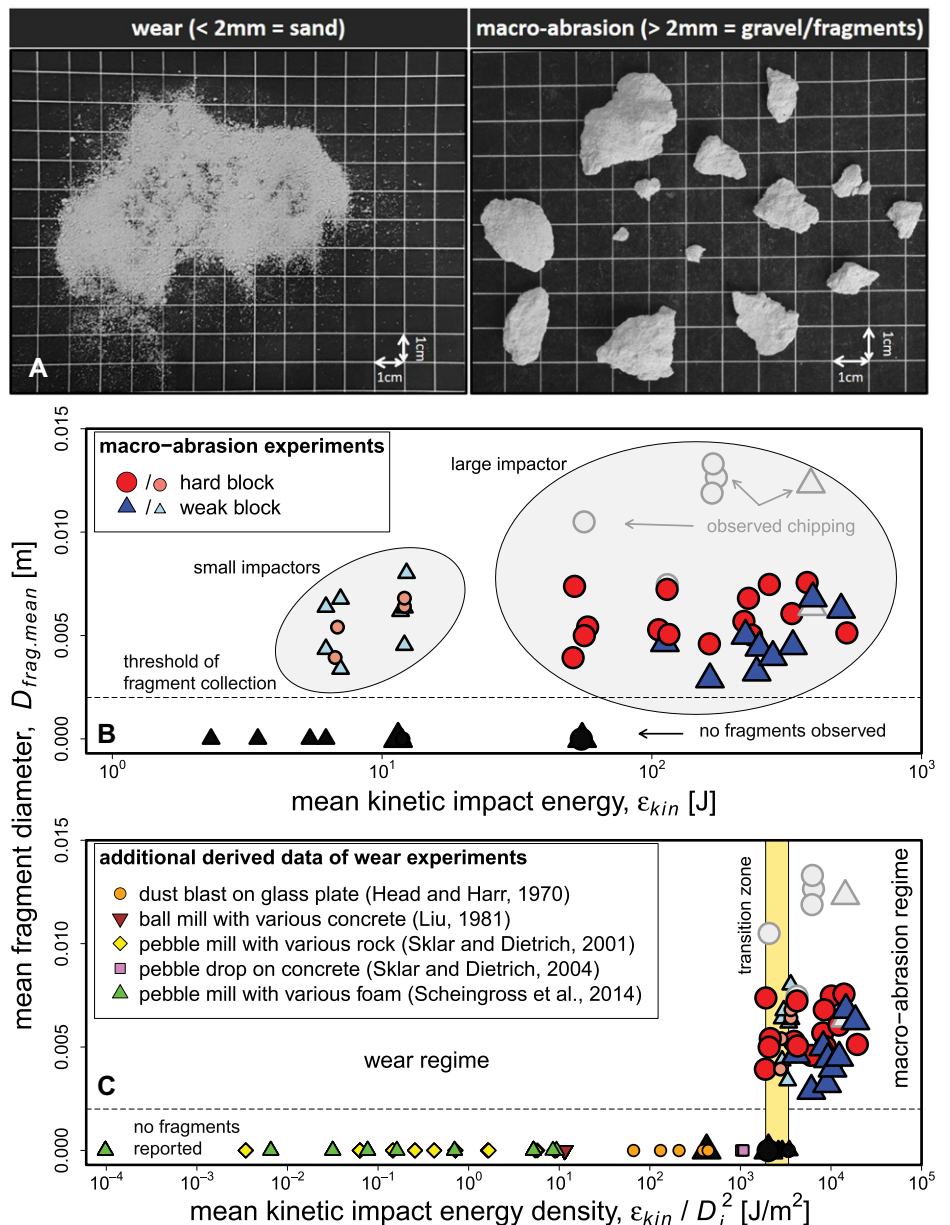

Figure 2. Bedrock abrasion regimes. (A) Examples of sand produced by wear (<2 mm) and fragments produced by macro-abrasion (on average 10 per experiment). (B) Mean fragment diameter, $D_{frag.mean}$, versus mean kinetic impact energy, ε_{kin}, for two clusters of impactor sizes. (C) $D_{frag.mean}$ versus impact energy density (ε_{kin} divided by squared impactor diameter, D_i^2), and calculated impact energy densities for prior experiments (Table S2 [see footnote 1]). Yellow area marks the transition to gravel-sized fragments; dark symbols indicate drop tests without fragment production (only wear). Some larger fragments chipped from protrusions late in the experiments after some slab topography evolved (light-gray shaded symbols); these were neglected from further analysis.

in rivers, we compiled a database of reported riverbed slopes, S, and water flow depths, H, from natural bedrock river sections (Table S3) and estimated the kinetic impact energy, ε_{imp}, for their median transportable grain sizes, D_{50} (see the Supplemental Material).

RESULTS

Most of the impact energy was consumed plastically by damaging the rock slabs, with only 5% ($\pm 4\%$) remaining in the rebounding grains, so $\varepsilon_{kin} = \varepsilon_{imp}$. In low-impact-energy experiments (<5 J), abraded fragments resembled the 0.2 mm concrete-constituent sand particles, consistent with wear. However, with increasing impact energy, we observed a transition to gravel-sized fragments with diameters >2 mm and ranging up to 20 mm in their B axis (Fig. 2A) being of general platelet shape (Fig. S2). We used the sand-gravel boundary diameter of 2 mm as an arbitrary fragment reference size for the onset of macro-abrasion, because it is 10-fold larger than the concrete's sand size (i.e., it was not grain-by-grain wear; Whipple, 2004). The onset of macro-abrasion was similar between the hard and weak rock slabs, but it differed with impactor size, where smaller impactors produced gravel fragments at smaller impact energies (Fig. 2B). These data collapsed when the impact energy was normalized by the square of the impactor diameter, D_i^2 (Fig. 2C), which might be a reasonable proxy for kinetic impact energy density (i.e., ε_{kin} normalized by the impact area). A narrow zone of ε_{kin}/D_i^2 (1.9–3.4 kJ/m^2) well defines the transition to gravel-sized fragments, irrespective of the exact reference diameter and consistent with previous experiments producing smaller fragments (Fig. 2C).

Despite the change in erosion behavior from wear to macro-abrasion, total abrasion volume did not change significantly across this transition, and it was not dependent on impactor size. Instead, our results match those from previous work in which the abrasion volume per impact, V_a, scales as $V_a \propto \varepsilon_{kin}/\sigma_t^2$ over 13 orders of magnitude (Fig. 3). Higher abrasion volumes in the macro-abrasion regime occurred by producing more numerous rather than larger fragments (Fig. S3).

DISCUSSION

Macro-abrasion in our experiments likely occurred by dissipative plastic deformation (i.e., brittle wear; Bitter, 1963), expressed in surface-parallel tensile failure and spalling of platelets (Fig. 2A; Fig. S2; Lange et al., 1984; Polanskey and Ahrens, 1990). We expect the earlier onset of gravel-sized fragments for the small impactors was due to higher energy density (focused impact energy into a smaller contact area; Fig. 2C), resulting in larger fractures developing. We did not observe macro-abrasion to occur more readily or produce larger fragments

for the more brittle, higher-tensile-strength concrete. However, our experiments only spanned a factor of ~2 in σ_t, and future work may reveal a rock-strength effect on fragment size. We found a slight increase in average fragment size with increasing ε_{kin} (Fig. 2C); this is counter to the size decrease with increasing ε_{kin} observed for much higher-energy impact and explosion experiments with dynamic fragmentation (Grady and Kipp, 1985; Hogan et al., 2012).

Abrasion volume, V_a, in the macro-abrasion regime scaled similar as in the wear regime and is a linear function of $\varepsilon_{kin}/\sigma_t^2$ (Fig. 3). The tested range of impact energies also is similar to natural bedrock rivers, thereby validating mechanistic models for fluvial abrasion (Head and Harr, 1970; Sklar and Dietrich, 2004; Lamb et al., 2008; Scheingross et al., 2014) for both abrasion regimes. Others have proposed a logarithmic relation between V_a and $\varepsilon_{kin}/\sigma_t^2$ to account for a threshold energy needed to initiate fracture (Hogan et al., 2012). However, our results do not support a threshold, suggesting abrasion occurs by bedrock fatigue, i.e., cumulative growing and intersecting fractures even from very small ε_{kin} (Hogan et al., 2012; Hutchings and Shipway, 2017); though, we cannot rule out preconditioning in some of our experiments. The angularity
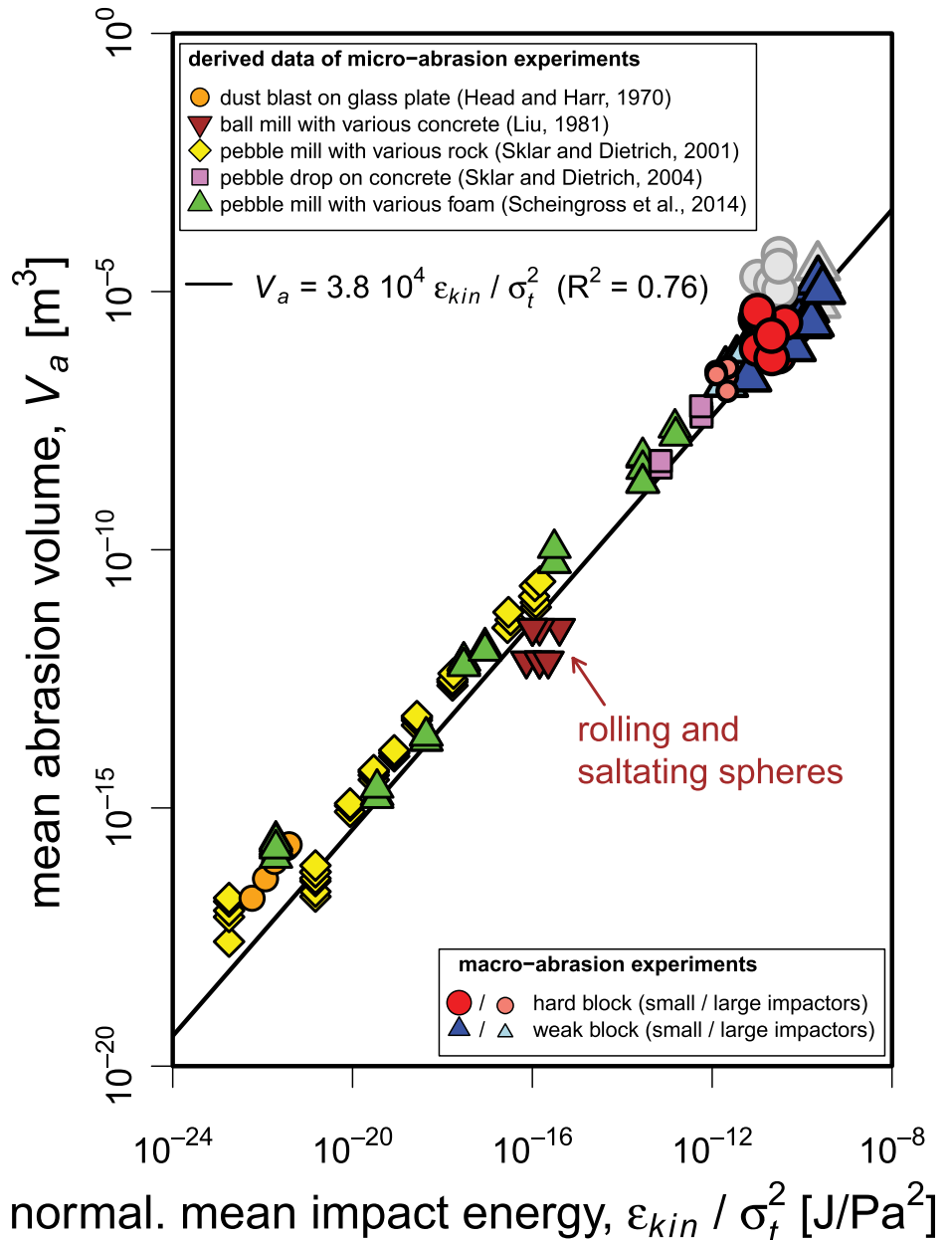

Figure 3. Bedrock erodibility over 13 orders of magnitude: mean total abrasion volume, V_a, versus normalized mean kinetic impact energy (i.e., ε_{kin} divided by squared tensile strength σ_t^2; Table S2 [see footnote 1]). Brown triangles show abrasion mill experiments with mostly rolling steel balls; light gray-shaded data in macro-abrasion experiments are from chipping and were excluded from regression.
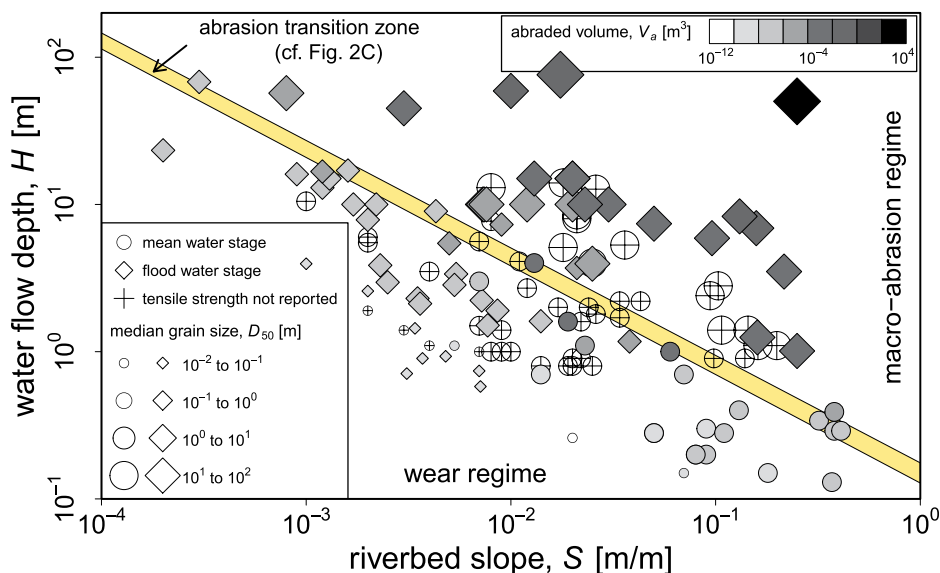
Figure 4. Bedrock river erosivity framework based on bed slope, *S*, and flow depth, *H*. Data come from previously reported mean or flood flow depths (circles or diamonds; Table S3 [see footnote 1]). Point size reflects median transportable grain size, D_{50}. Shading indicates abraded volume, V_a, based on normalized grain impact energy $\varepsilon_{kin}/\sigma_t^2$, if σ_t values were available (crossed symbols otherwise). Yellow shaded area marks the transition from wear to macro-abrasion regime, based on impact energy density, $\varepsilon_{kin}/D_{50}^2$, for the generation of gravel-sized fragments in our experiments (cf. Fig. 2C).

of impacting grains also conditions abrasion (Engel, 1978), as evident from the lower erosivity of mostly rolling and sliding steel balls (brown triangles in Fig. 3; Liu, 1981). We would expect the relation $V_a \propto \varepsilon_{kin}/\sigma_t^2$ to hold for any rock abrasion process driven by impacts, including erosion by debris flows (Stock and Dietrich, 2006), wave attack on coastal platforms (Cullen and Bourke, 2018), rock fall, and eolian abrasion (Anderson, 1986).

While our experiments were designed to simulate impacts into a flat bed, we observed larger fragments and higher abrasion rates due to rock chipping at surface protrusions (Wilson and Lavé, 2014) that developed in the rock slab's center as some experiments progressed (gray shaded data in Figs. 2B and 2C; Fig. 3). Wear in rivers tends to smooth topography into convex surfaces (Hancock et al., 1998), which may inhibit chipping. However, for many rock types, abundant irregularities and preexisting fractures (Scott and Wohl, 2019) likely promote chipping. Moreover, large instantaneous rock abrasion from a single boulder impact can create significant bedrock roughness (Fig. 4; Wende, 1999) and damage the surrounding rock (Tinkler, 1993). Increased bedrock roughness might in turn promote feedbacks with flow turbulence, the spatial distribution of bed-load impacts and cover, and therefore influence channel evolution (Beer et al., 2017).

Based on the transition to macro-abrasion as a function of impact energy density (Fig. 2C), we defined an erosivity framework applicable to natural rivers (Fig. 4). The generation of 2 mm fragments is an arbitrary

reference value for macro-abrasion, but it is useful for natural rivers. It is the boundary between sand- and gravel-sized fragments, sand, and silt that often constitute wash load in mountain rivers, and most natural rocks are composed of sand-sized or smaller mineral grains; therefore, these factors comply with the definition of wear (Whipple, 2004). Calculated grain impact energies from 125 bedrock river reaches spanned 14 orders of magnitude (10^{-2} to 10^{11} J), and almost 40% of them fell into the predicted macro-abrasion regime (Table S3). This corresponds to rivers capable of transporting coarse sediment ($D_{50} > 0.6$ m) that can produce high impact energies (>1 kJ), stemming from large flow depths or steep slopes. Using estimates of σ_t, rivers in the macro-abrasion regime also showed the highest expected abrasion volumes per impact (exceeding 1 m³ in some cases; Fig. 4; Table S3). Thus, while it is known that plucking in fractured rock can remove blocks meters in scale (Miller, 1991; Wende, 1999; Whipple et al., 2000; Lamb and Fonstad, 2010; Anton et al., 2015), comparable instantaneous erosion amounts might also occur in massive rock due to macro-abrasion (Tinkler, 1993; Hancock et al., 1998; Hartshorn et al., 2002; Beer et al., 2017).

CONCLUSIONS

We conducted impact experiments on a concrete bed to explore abrasion mechanics using high grain impact energies similar to those in mountain rivers. The transition from the wear to the macro-abrasion regime, here

defined as the generation of >2-mm-diameter fragments, occurred around an impact energy density threshold of 1 kJ/m². Despite the differences in fragment sizes generated in our experiments, the total volumetric abrasion rate followed the same scaling law with impact energy as in wear experiments, validating usage of a general abrasion mode for high impact energies in massive rock. However, erosion rates were larger where bedrock chipping occurred at topographic protrusions developed by macro-abrasion. We found that most (95%) of the impactor's kinetic energy was spent on abrasion work during the impact process; thus, the common approximation of $\varepsilon_{kin} \sim \varepsilon_{imp}$ appears to be valid. Many natural bedrock rivers are likely in the macro-abrasion regime, specifically those capable of transporting boulders ($D_{50} > 0.6$ m). In these rivers, even single impacts can cause significant topographic change and may drive morphodynamic feedbacks differing from those in the wear regime.

REFERENCES CITED
Anderson, R.S., 1986, Erosion profiles due to particles entrained by wind: Application of an eolian sediment transport model: Geological Society of America Bulletin, v. 97, p. 1270–1278, https://doi.org/10.1130/0016-7606(1986)97<1270:EPDTPE>2.0.CO;2.

Anton, L., Mather, A.E., Stokes, M., Munoz-Martin, A., and De Vicente, G., 2015, Exceptional river gorge formation from unexceptional floods: Nature Communications, v. 6, p. 7963–7963, https://doi.org/10.1038/ncomms8963.

Atkinson, B.K., 1987, Fracture Mechanics of Rock: New York, Elsevier Scientific, 534 p., https://doi.org/10.1016/C2009-0-21691-6.

Beer, A.R., Turowski, J.M., and Kirchner, J.W., 2017, Spatial patterns of erosion in a bedrock gorge: Journal of Geophysical Research: Earth Surface, v. 122, p. 191–214, https://doi.org/10.1002/2016JF003850.

Bitter, J.G.A., 1963, A study of erosion phenomena, part I: Wear, v. 6, p. 5–21, https://doi.org/10.1016/0043-1648(63)90003-6.

Chatanantavet, P., and Parker, G., 2009, Physically-based modeling of bedrock incision by abrasion, plucking, and macroabrasion: Journal of Geophysical Research, v. 114, F04018, https://doi.org/10.1029/2008JF001044.

Cullen, N.D., and Bourke, M.C., 2018, Clast abrasion of a rock shore platform on the Atlantic coast of Ireland: Earth Surface Processes and Landforms, v. 43, p. 2627–2641, https://doi.org/10.1002/esp.4421.

Engel, P.A., 1978, Impact Wear of Materials: New York, Elsevier Scientific, 339 p., https://doi.org/10.1115/1.3424343.

Grady, D.E., and Kipp, M.E., 1985, Mechanisms of dynamic fragmentation: Factors governing fragment size: Mechanics of Materials, v. 4, p. 311–320, https://doi.org/10.1016/0167-6636(85)90028-6.

Hancock, G.S., Anderson, R.S., and Whipple, K.X., 1998, Beyond power: Bedrock river incision process and form, in Tinkler, K.J., and Wohl, E.E., eds., Rivers Over Rock: Fluvial Processes in Bedrock Channels: American Geophysical Union Geophysical Monograph 107, p. 35–60, https://doi.org/10.1029/GM107p0035.

Hartshorn, K., Hovius, N., Dade, W.B., and Slingerland, R.L., 2002, Climate-driven bedrock incision in an active mountain belt: Science, v. 297, p. 2036–2038, https://doi.org/10.1126/science.1075078.

Head, W.J., and Harr, M.E., 1970, The development of a model to predict the erosion of materials by natural contaminants: Wear, v. 15, p. 1–46, https://doi.org/10.1016/0043-1648(70)90184-5.

Hogan, J.D., Rogers, R.J., Spray, J.G., and Boonsu, S., 2012, Dynamic fragmentation of granite for impact energies of 6–28 J: Engineering Fracture Mechanics, v. 79, p. 103–125, https://doi.org/10.1016/j.engfracmech.2011.10.006.

Hutchings, I.M., and Shipway, P., 2017, Tribology: Friction and Wear of Engineering Materials: New York, Elsevier Scientific, 412 p.

Lague, D., 2010, Reduction of long-term bedrock incision efficiency by short-term alluvial cover intermittency: Journal of Geophysical Research, v. 115, F02011, https://doi.org/10.1029/2008JF001210.

Lamb, M.P., and Fonstad, M.A., 2010, Rapid formation of a modern bedrock canyon by a single flood event: Nature Geoscience, v. 3, p. 477–481, https://doi.org/10.1038/ngeo894.

Lamb, M.P., Dietrich, W.E., and Sklar, L.S., 2008, A model for fluvial bedrock incision by impacting suspended and bedload sediment: Journal of Geophysical Research: Earth Surface, v. 113, F03025, https://doi.org/10.1029/2007JF000915.

Lamb, M.P., Finnegan, N.J., Scheingross, J.S., and Sklar, L.S., 2015, New insights into the mechanics of fluvial bedrock erosion through flume experiments and theory: Geomorphology, v. 244, p. 33–55, https://doi.org/10.1016/j.geomorph.2015.03.003.

Lange, M.A., Ahrens, T.J., and Boslough, M.B., 1984, Impact cratering and spall failure of gabbro: Icarus, v. 58, p. 383–395, https://doi.org/10.1016/0019-1035(84)90084-8.

Liu, T.C., 1981, Abrasion resistance of concrete: ACI (American Concrete Institute) Journal, v. 78, p. 341–350.

Miller, J.R., 1991, The influence of bedrock geology on knickpoint development and channel-bed degradation along downcutting streams in south-central Indiana: The Journal of Geology, v. 99, p. 591–605, https://doi.org/10.1086/629519.

Polanskey, C.A., and Ahrens, T.J., 1990, Impact spallation experiments: Fracture patterns and spall velocities: Icarus, v. 87, p. 140–155, https://doi.org/10.1016/0019-1035(90)90025-5.

Scheingross, J.S., Brun, F., Lo, D., Omerdin, K., and Lamb, M.P., 2014, Experimental evidence for fluvial bedrock incision by suspended and bedload sediment: Geology, v. 42, p. 523–526, https://doi.org/10.1130/G35432.1.

Scott, D., and Wohl, E.E., 2019, Bedrock fracture influences on geomorphic process and form across process domains and scales: Earth Surface Processes and Landforms, v. 44, p. 27–45, https://doi.org/10.1002/esp.4473.

Sklar, L.S., and Dietrich, W.E., 2001, Sediment and rock strength controls on river incision into bedrock: Geology, v. 29, p. 1087–1090, https://doi.org/10.1130/0091-7613(2001)029<1087:SARSCO>2.0.CO;2.

Sklar, L.S., and Dietrich, W.E., 2004, A mechanistic model for river incision into bedrock by saltating bed load: Water Resources Research, v. 40, W06301, https://doi.org/10.1029/2003WR002496.

Small, E.E., Blom, T., Hancock, G.S., Hynek, B.M., and Wobus, C.W., 2015, Variability of rock erodibility in bedrock-floored stream channels based on abrasion mill experiments: Journal of Geophysical Research: Earth Surface, v. 120, p. 1455–1469, https://doi.org/10.1002/2015JF003506.

Stock, J.D., and Dietrich, W.E., 2006, Erosion of steepland valleys by debris flows: Geological Society of America Bulletin, v. 118, p. 1125–1148, https://doi.org/10.1130/B25902.1.

Tinkler, K.J., 1993, Fluvially sculpted rock bedforms in Twenty Mile Creek, Niagara Peninsula, Ontario: Canadian Journal of Earth Sciences, v. 30, p. 945–953, https://doi.org/10.1139/e93-079.

Turowski, J.M., Boeckli, M., Rickenmann, D., and Beer, A.R., 2013, Field measurements of the energy delivered to the channel bed by moving bed load and links to bedrock erosion: Journal of Geophysical Research: Earth Surface, v. 118, p. 2438–2450, https://doi.org/10.1002/2013JF002765.

Turowski, J.M., Wyss, C., and Beer, A.R., 2015, Grain size effects on energy delivery to the stream bed and links to bedrock erosion: Geophysical Research Letters, v. 42, p. 1775–1780, https://doi.org/10.1002/2015GL063159.

Wende, R., 1999, Boulder bedforms in jointed-bedrock channels, in Miller, A.J., and Gupta, A., eds., Varieties of Fluvial Form: Chichester, UK, Wiley, p. 189–216.

Whipple, K.X., 2004, Bedrock rivers and the geomorphology of active orogens: Annual Review of Earth and Planetary Sciences, v. 32, p. 151–185, https://doi.org/10.1146/annurev.earth.32.101802.120356.

Whipple, K.X., Hancock, G.S., and Anderson, R.S., 2000, River incision into bedrock: Mechanics and relative efficacy of plucking, abrasion, and cavitation: Geological Society of America Bulletin, v. 112, p. 490–503, https://doi.org/10.1130/0016-7606(2000)1120490:RIIBMA>2.3.CO;2.

Wilson, A., and Lavé, J.Ô., 2014, Convergent evolution of abrading flow obstacles: Insights from analogue modelling of fluvial bedrock abrasion by coarse bedload: Geomorphology, v. 208, p. 207–224, https://doi.org/10.1016/j.geomorph.2013.11.024.